

hep-ph/0304077
DO-TH 02/21
OSU-HEP-03-03
DESY 03-046
April 2003

Standard Model CP violation in Polarised $b \rightarrow dl^+l^-$

K.S. Babu¹

*Department of Physics, Oklahoma State University, Stillwater, OK 74078,
U.S.A.*

K.R.S. Balaji²,

*Institut für Theoretische Physik, Universität Dortmund, 44221 Dortmund,
Germany*

and

I. Schienbein³

DESY/Univ. Hamburg, Notkestrasse 85, 22603 Hamburg, Germany

Abstract

In the standard model, we study CP violating rate asymmetries in the decay $b \rightarrow dl^+l^-$ when one of the leptons is polarised. We find an asymmetry of $(5 \div 15)\%$ in the polarised decay spectrum which is comparable to known results for the unpolarised case. In the kinematic region separating the $\rho - \omega$ and $c\bar{c}$ resonances, which is also theoretically cleanest, the polarised contribution to the asymmetry is larger than the unpolarised results. In order to observe a 3σ signal for direct CP violation in the polarised spectrum, assuming 100% efficiency, about 10^{10} $B\bar{B}$ pairs are required at a B factory. Our results indicate an asymmetric contribution from the individual polarisation states to the unpolarised CP asymmetry. Taking advantage of this, one can attribute any new physics to be most sensitive to a specific polarisation state.

¹babu@hep.phy.okstate.edu

²balaji@zylon.physik.uni-dortmund.de

³schien@mail.desy.de

1 Introduction

Flavor changing neutral current decays are important probes for new physics beyond the standard model (SM) [1]. Such currents are absent in the SM at the tree level and their strength is small at the one-loop level due to the GIM mechanism [2]. Furthermore, such transitions can also be CKM suppressed in the SM. Hence, in such decays, any enhancement over the SM expectations is an unambiguous signature for new physics. In this direction, the first observations of the radiative B decays ($B \rightarrow X_s \gamma$) by CLEO [3] and later by ALEPH [4] have yielded $|V_{ts}V_{tb}^*| \sim 0.035$ which is in conformity with the CKM estimates. However, in radiative decay modes, deviations from SM predictions are sensitive to the photon spectrum which poses considerable experimental difficulties, in particular, measuring the lower end of the spectrum [5]. In parallel, rare semi-leptonic decays ($b \rightarrow ql^+l^-$) can provide alternative sources to discover new physics and these are relatively cleaner than pure hadronic decays. The semi-leptonic decays are induced by strong interaction corrected effective Hamiltonians and the matrix elements receive the dominant contributions from loops with virtual top quarks and weak bosons which are proportional to $V_{tb}V_{tq}^*$ with $q = d, s$. In such decays, the standard observables such as lepton polarization asymmetries, forward-backward asymmetry and also CP violation can be studied kinematically as a function of the invariant di-lepton mass. Within the SM, the semi-leptonic process has earlier been studied by a number of authors [6].

In the SM, for the decay $B \rightarrow X_q l^+ l^-$, the dominant contribution is from the parton level process $b \rightarrow ql^+l^-$ and is defined in terms of a set of ten effective operators $O_1 - O_{10}$ [7]. To be specific, we shall take $q = d$, and the truncated operator basis is reduced to the following five operators [8] given to be

$$\begin{aligned}
 O_1 &= (\bar{d}_L^\alpha \gamma_\mu b_L^\alpha)(\bar{c}_L^\beta \gamma^\mu c_L^\beta), \\
 O_2 &= (\bar{d}_L^\alpha \gamma_\mu b_L^\beta)(\bar{c}_L^\alpha \gamma^\mu c_L^\beta), \\
 O_7 &= (\bar{d}^\alpha \sigma_{\mu\nu} [m_b P_R + m_d P_L] b^\alpha) F^{\mu\nu}, \\
 O_9 &= (\bar{d}_L^\alpha \gamma_\mu b_L^\alpha)(\bar{l} \gamma^\mu l), \\
 O_{10} &= (\bar{d}_L^\alpha \gamma_\mu b_L^\alpha)(\bar{l} \gamma^\mu \gamma_5 l),
 \end{aligned} \tag{1}$$

and the additional operators [9]

$$\begin{aligned} O_1^u &= (\bar{d}_L^\alpha \gamma_\mu u_L^\beta)(\bar{u}_L^\beta \gamma^\mu b_L^\alpha), \\ O_2^u &= (\bar{d}_L^\alpha \gamma_\mu u_L^\alpha)(\bar{u}_L^\beta \gamma^\mu b_L^\beta). \end{aligned} \quad (2)$$

In the presence of new physics, there can be new tree level operators due to possible right-handed current-current operators and also operators involving SUSY scalar particles [10]. In this analysis, we do not consider them and will limit to the interactions determined by the SM.

Prior to the advent of the B factories such as BaBar and Belle the best experimental limits for the inclusive branching ratios $BR(b \rightarrow sl^+l^-)$ with $l = e, \mu$ as measured by CLEO [11] have been an order higher than the SM estimates [12]. Recently, the first measurement of this decay has been reported by Belle [13] and is in agreement with the SM expectations and hence further constrains any extensions to the SM. In this context, it is pertinent to exploit the features of the SM which makes it most sensitive to new physics. It has been argued that measuring the various lepton polarizations provides for a comprehensive test of the SM and further can be indicative of new physics [14].

In this exercise, we examine the SM contribution to CP violating effects for the case when one of the leptons is observed in a polarised state. As it turns out, the CP asymmetry is comparable to the unpolarised SM expectations when the lepton is in a specific polarised state. In other words, the net unpolarised CP asymmetry (which is a linear sum of the polarised asymmetries) receives unequal contributions from the individual polarised state. This feature can provide for measurements involving new physics search. Note that this conclusion, which is dependent on a specific polarisation state of the lepton is apriori not obvious from the operator structure given in (1); albeit, is well motivated from the observation that the electroweak sector of the SM is polarised (left-handed). Therefore, measurements of decay spectra when one of the final state lepton is in the *wrong sign* polarised state will be a key observable to any new physics. By *wrong sign* polarised state, we mean a lepton with a given polarisation, whose SM decay width is smaller when compared to the unpolarised spectrum.

Our paper is organized as follows. In the next section, we revise the basic theoretical framework and describe various observables such as decay spectra for polarised and unpolarised leptons and polarisation asymmetries. In order to be self contained, we have updated the known results by recalculating all

of the existing results taking care of the various theoretical issues involved. In section 3, we derive the CP violating decay rate asymmetries for polarised final state leptons and compare this with the CP violating asymmetry in the unpolarised case. In section 4, we present our numerical results and estimate the feasibility of measuring the CP violation in a B factory. Finally, in section 5, we conclude with a summary of the main results.

2 Theoretical framework

In this section, we describe our procedure for obtaining the decay spectra. We first perform a detailed analysis and rederive the known parton level results. In doing so, we try to clarify some of the theoretical uncertainties which go as input parameters for our numerical estimates. Our purpose is to ensure that our conclusions have subsumed some of these theoretical difficulties and also to complement the existing literature.

The QCD corrected effective Hamiltonian describing the decay $b \rightarrow dl^+l^-$ in the SM leads to the matrix element [9, 15]

$$M = \frac{G_F \alpha V_{tb} V_{td}^*}{\sqrt{2}\pi} \left[C_9^{\text{eff}} (\bar{d}\gamma_\mu P_L b) \bar{l}\gamma^\mu l + C_{10} (\bar{d}\gamma_\mu P_L b) \bar{l}\gamma^\mu \gamma^5 l - 2C_7^{\text{eff}} \bar{d}i\sigma_{\mu\nu} \frac{q^\nu}{q^2} (m_b P_R + m_d P_L) b \bar{l}\gamma^\mu l \right], \quad (3)$$

where the notations employed are the standard ones and q denotes the four momentum of the lepton pair. In the SM, except for C_9^{eff} , the Wilson couplings are real and analytic expressions can be found in the literature [15, 16, 17]. The numerical values of the Wilson coefficients depend on five parameters ($\mu, m_t, m_W, \sin^2 \theta_W, \alpha_s(M_Z)$) which are listed in the appendix of this paper. For a consistent NLO analysis all the coefficients, except C_9 , should be calculated in the leading log approximation; see [15] for a detailed explanation. We obtain these to be,

$$\begin{aligned} C_7^{\text{eff}} &= -0.310, & C_{10} &= -4.181, & C_1 &= -0.251, & C_2 &= 1.108 \\ C_3 &= 1.120 \times 10^{-2}, & C_4 &= -2.584 \times 10^{-2}, & C_5 &= 7.443 \times 10^{-3}, & & \\ C_6 &= -3.167 \times 10^{-2}, & C_9^{\text{NDR}} &= 4.128. & & & & \end{aligned} \quad (4)$$

We place a few remarks here. The above numbers differ from the ones used in [9] and we attribute the main source of this difference in the use of the $\overline{\text{MS}}$

top quark mass $m_t = 165$ GeV [15] instead of a pole mass of $m_t = 176$ GeV. It is noteworthy that the leading log results have been obtained utilizing a two-loop $(\overline{\text{MS}})$ α_s with $\alpha_s(M_Z^2) = 0.1183$. Using a leading order α_s with $\alpha_s^{\text{LO}}(M_Z^2) = 0.130$ as obtained by the CTEQ collaboration from a global LO analysis of parton distribution functions [18] results in marginal changes, e.g., $C_1 = -0.261$, $C_2 = 1.114$, $C_7^{\text{eff}} = -0.314$. The value of $C_9 \equiv C_9^{\text{NDR}}$ has been obtained at NLO accuracy in the NDR scheme. On the other hand, the effective coefficient C_9^{eff} is scheme independent. It can be parametrized in the following way [9]:

$$C_9^{\text{eff}} = \xi_1 + \lambda_u \xi_2, \quad \lambda_u = \frac{V_{ub}V_{ud}^*}{V_{tb}V_{td}^*}, \quad (5)$$

with

$$\begin{aligned} \xi_1 = & C_9 + 0.138 \omega(\hat{s}) + g(\hat{m}_c, \hat{s})(3C_1 + C_2 + 3C_3 + C_4 + 3C_5 + C_6) \\ & - \frac{1}{2}g(\hat{m}_d, \hat{s})(C_3 + C_4) - \frac{1}{2}g(\hat{m}_b, \hat{s})(4C_3 + 4C_4 + 3C_5 + C_6) \\ & + \frac{2}{9}(3C_3 + C_4 + 3C_5 + C_6), \end{aligned} \quad (6)$$

$$\xi_2 = [g(\hat{m}_c, \hat{s}) - g(\hat{m}_u, \hat{s})](3C_1 + C_2). \quad (7)$$

Here, $\hat{s} = q^2/m_b^2$ and $\hat{m}_q = m_q/m_b$ are dimensionless variables scaled with respect to the bottom quark mass. Note that some of the Wilson coefficients in (4) entering (6) and (7) are small and/or add up destructively in such a way that the functions $\xi_{1,2}$ in the NLO approximation give the following simple expressions,

$$\xi_1 \simeq 4.128 + 0.138 \omega(\hat{s}) + 0.36 g(\hat{m}_c, \hat{s}), \quad \xi_2 \simeq 0.36 [g(\hat{m}_c, \hat{s}) - g(\hat{m}_u, \hat{s})]. \quad (8)$$

In (6), the function $\omega(\hat{s})$ represents one loop corrections to the operator O_9 [19] and the function $g(\hat{m}_q, \hat{s})$ represents the corrections to the four-quark operators $O_1 - O_6$ [17], i.e.,

$$\begin{aligned} g(\hat{m}_q, \hat{s}) = & -\frac{8}{9} \ln(\hat{m}_q) + \frac{8}{27} + \frac{4}{9} y_q - \frac{2}{9}(2 + y_q)\sqrt{|1 - y_q|} \left\{ \Theta(1 - y_q) \times \right. \\ & \left. \left[\ln \left(\frac{1 + \sqrt{1 - y_q}}{1 - \sqrt{1 - y_q}} \right) - i\pi \right] + \Theta(y_q - 1) 2 \arctan \frac{1}{\sqrt{y_q - 1}} \right\}, \end{aligned} \quad (9)$$

with $y_q \equiv 4\hat{m}_q^2/\hat{s}$.

In addition to the short distance contributions described above, the decays $B \rightarrow X_d l^+ l^-$ also receive long distance contributions from the tree-level diagrams involving $u\bar{u}$, $d\bar{d}$, and $c\bar{c}$ bound states, $B \rightarrow X_d(\rho, \omega, J/\psi, \psi', \dots) \rightarrow X_d l^+ l^-$. These effects can be taken into account by modifying the functions $g(\hat{m}_q, \hat{s})$. In the case of the J/Ψ family these pole contributions can be incorporated by employing a Breit-Wigner form for the resonance states [6, 20] through the replacement

$$g(\hat{m}_c, \hat{s}) \rightarrow g(\hat{m}_c, \hat{s}) - \frac{3\pi}{\alpha^2} \sum_{V=J/\psi, \psi', \dots} \frac{M_V Br(V \rightarrow l^+ l^-) \Gamma_{all}^V}{s - M_V^2 + i\Gamma_{all}^V M_V}. \quad (10)$$

In (10), the sum includes all $c\bar{c}$ bound states V with mass M_V and total width Γ_{all}^V . The $c\bar{c}$ long distance contributions to the branching fraction are obviously dominant near the J/ψ resonance peak. In addition to this, there can be long distance contributions from real $u\bar{u}$, $d\bar{d}$ quark pairs giving rise to intermediate vector meson states, i.e., ρ and ω . In many of the existing analysis performed so far, these resonance contributions have been neglected. A plausible reason being, in the decays $B \rightarrow X_s l^+ l^-$ they are CKM suppressed. However, in [9] it has been demonstrated that the ρ and ω resonances contribute quite sizeably to the CP violating decay rate asymmetry and should be taken into account in theoretical studies of this observable.

Following the approach in [9, 21] we calculate the functions $g(\hat{m}_u, \hat{s})$, $g(\hat{m}_d, \hat{s})$ and $g(\hat{m}_c, \hat{s})$ using a dispersive method. To be precise, $g(\hat{m}_u, \hat{s})$ and $g(\hat{m}_d, \hat{s})$ have been calculated exactly along the lines described in [9, 21] using quark masses $m_u = m_d = m_\pi$. Concerning $g(\hat{m}_c, \hat{s})$, the continuous part has been computed with the dispersive method as well whereas, for simplicity, the $c\bar{c}$ resonances have been evaluated according to (10). Finally, the function $g(\hat{m}_b, \hat{s})$ has been evaluated with help of (9). Note that the contribution of $g(\hat{m}_b, \hat{s})$ to C_9^{eff} in (5) is negligible.

2.1 Unpolarized decay spectrum

In the absence of low energy QCD corrections ($\sim 1/m_b^2$) [22, 12] and setting the down quark mass to zero, the unpolarized differential decay width as a function of the invariant mass of the lepton pair is

$$\frac{d\Gamma}{d\hat{s}} = \frac{G_F^2 m_b^5 \alpha^2}{768\pi^5} |V_{tb} V_{td}^*|^2 \lambda^{\frac{1}{2}}(1, \hat{s}, 0) a \Delta(\hat{s}); \quad a \equiv \sqrt{1 - \frac{4\hat{m}_l^2}{\hat{s}}}. \quad (11)$$

In (11), the triangle function λ is given $\lambda(a, b, c) = a^2 + b^2 + c^2 - 2(ab + bc + ca)$ and the kinematic factors are

$$\begin{aligned}
\Delta(\hat{s}) &= \left[12\text{Re}(C_7^{\text{eff}} C_9^{\text{eff}*}) F_1(\hat{s}) + \frac{4}{\hat{s}} |C_7^{\text{eff}}|^2 F_2(\hat{s}) \right] \left(1 + \frac{2\hat{m}_l^2}{\hat{s}} \right) \\
&\quad + (|C_9^{\text{eff}}|^2 + |C_{10}|^2) F_3(\hat{s}) + 6\hat{m}_l^2 (|C_9^{\text{eff}}|^2 - |C_{10}|^2) F_1(\hat{s}) , \\
F_1(\hat{s}) &= 1 - \hat{s} , \\
F_2(\hat{s}) &= 2 - \hat{s} - \hat{s}^2 , \\
F_3(\hat{s}) &= 1 + \hat{s} - 2\hat{s}^2 + \lambda(1, \hat{s}, 0) \frac{2\hat{m}_l^2}{\hat{s}} . \tag{12}
\end{aligned}$$

The various quantities in the above differential decay width are scaled with respect to the b quark mass m_b and are indicated by a hat. The physical range for \hat{s} is given by $4\hat{m}_l^2 \leq \hat{s} \leq 1$ as is dictated by the threshold factor, a , and the triangle function in (11). The above differential spectrum has been obtained earlier by Krüger et al., [21, 9] (for $m_l \neq 0$ and $m_q \neq 0$), Ali et al., [23, 24] (for $m_l = 0$), Grinstein et al., [8], Buras et al., [15] (for $m_q = 0$ and $m_l = 0$) and by Hewett [25] (for $m_q = 0$, which agrees with our expressions).

As usual we remove uncertainties in (11) due to the b quark mass (a factor of m_b^5) by introducing the charged current semi-leptonic decay rate

$$\Gamma(B \rightarrow X_c e \bar{\nu}_e) = \frac{G_F^2 m_b^5}{192\pi^3} |V_{cb}|^2 f(\hat{m}_c) \kappa(\hat{m}_c) \tag{13}$$

where $f(\hat{m}_c)$ and $\kappa(\hat{m}_c)$ represent the phase space and the one-loop QCD corrections to the semi-leptonic decay and can be found in [9]. Therefore the differential branching ratio can be written as

$$\frac{d\Gamma}{d\hat{s}} = \frac{\alpha^2}{4\pi^2} \frac{|V_{tb} V_{td}^*|^2}{|V_{cb}|^2} \frac{B(B \rightarrow X_c e \bar{\nu}_e)}{f(\hat{m}_c) \kappa(\hat{m}_c)} \lambda^{\frac{1}{2}}(1, \hat{s}, 0) a \Delta(\hat{s}) . \tag{14}$$

2.2 Polarized decay spectrum

The lepton polarisation has been first analyzed by Hewett [25] and Krüger and Sehgal [21] who showed that additional information can be obtained on the quadratic functions of the effective Wilson couplings, C_7^{eff} , C_{10} and C_9^{eff} . In order to calculate the polarised decay spectrum, one defines a reference

frame with three orthogonal unit vectors \mathbf{e}_L , \mathbf{e}_N and \mathbf{e}_T , such that

$$\begin{aligned}\mathbf{e}_L &= \frac{\mathbf{p}_{l^-}}{|\mathbf{p}_{l^-}|}, \\ \mathbf{e}_N &= \frac{\mathbf{p}_q \times \mathbf{p}_{l^-}}{|\mathbf{p}_q \times \mathbf{p}_{l^-}|}, \\ \mathbf{e}_T &= \mathbf{e}_N \times \mathbf{e}_L,\end{aligned}\tag{15}$$

where \mathbf{p}_q and \mathbf{p}_{l^-} are the three momentum vectors of the quark and the l^- lepton, respectively, in the l^+l^- center-of-mass system. Given the lepton l^- spin direction \mathbf{n} , which is a unit vector in the l^- rest frame, the differential decay spectrum can be written as [21]

$$\frac{d\Gamma(\hat{s}, \mathbf{n})}{d\hat{s}} = \frac{1}{2} \left(\frac{d\Gamma(\hat{s})}{d\hat{s}} \right)_{\text{unpol}} \left[1 + (P_L \mathbf{e}_L + P_T \mathbf{e}_T + P_N \mathbf{e}_N) \cdot \mathbf{n} \right],\tag{16}$$

where the polarisation components P_L , P_N and P_T can be constructed as follows;

$$P_i(\hat{s}) = \frac{d\Gamma(\mathbf{n} = \mathbf{e}_i)/d\hat{s} - d\Gamma(\mathbf{n} = -\mathbf{e}_i)/d\hat{s}}{d\Gamma(\mathbf{n} = \mathbf{e}_i)/d\hat{s} + d\Gamma(\mathbf{n} = -\mathbf{e}_i)/d\hat{s}}, \quad i = L, N, T.\tag{17}$$

The resulting polarisation asymmetries are

$$\begin{aligned}P_L(\hat{s}) &= \frac{a}{\Delta(\hat{s})} \left[12\text{Re}(C_7^{\text{eff}} C_{10}^*) (1 - \hat{s}) + 2\text{Re}(C_9^{\text{eff}} C_{10}^*) (1 + \hat{s} - 2\hat{s}^2) \right], \\ P_T(\hat{s}) &= \frac{3\pi\hat{m}_l}{2\Delta(\hat{s})\sqrt{\hat{s}}} \lambda^{1/2}(1, \hat{s}, 0) \left[2\text{Re}(C_7^{\text{eff}} C_{10}^*) - 4\text{Re}(C_7^{\text{eff}} C_9^{\text{eff}*}) - \frac{4}{\hat{s}} |C_7^{\text{eff}}|^2 \right. \\ &\quad \left. + \text{Re}(C_9^{\text{eff}} C_{10}^*) - |C_9^{\text{eff}}|^2 \hat{s} \right], \\ P_N(\hat{s}) &= \frac{3\pi\hat{m}_l a}{2\Delta(\hat{s})} \lambda^{1/2}(1, \hat{s}, 0) \sqrt{\hat{s}} \text{Im}(C_9^{\text{eff}*} C_{10}),\end{aligned}\tag{18}$$

where we differ by a factor of 2 in P_T with respect to the results obtained in [21]. The above expressions for P_i agree with [10] for the SM case.

As can be seen, the polarisation asymmetries in (18) have different quadratic combinations of the Wilson couplings and any alteration in the values of these couplings can lead to changes in the asymmetries. Thus, these are sensitive to new physics and can also probe the relative signs of the couplings C_7^{eff} , C_9^{eff} and C_{10} . The normal polarisation asymmetry P_N is proportional

to $\text{Im}(C_9^{\text{eff}}C_{10}^*)$ and is thus sensitive to the absorptive part of the loop contributed by the charm quark.

The transverse and normal asymmetries P_T and P_N , respectively, are proportional to \hat{m}_l and thus the effects can be significant for the case of tau leptons. However, the case for tau leptons is an experimental challenge. One reason is that the tau decays in to final states with a neutrino and this involves uncertainties due to missing energy. Also, the predominant decays of the tau lepton are hadronic and this is an undesirable feature at hadronic colliders. Setting aside these problems, in our analysis, we illustrate the results when the final state lepton is an electron and tau; the results when a muon is produced are almost identical to the electron case.

3 CP violation

In the SM, CP violation in the decay $B \rightarrow X_s l^+ l^-$ is strongly suppressed. This follows from the unitarity of the CKM matrix. However, in the semi-leptonic B decay, $B \rightarrow X_d l^+ l^-$, the CP violating effects are not so strongly suppressed. The CP asymmetry for this decay can be observed by measuring the partial decay rates for the process and its charge conjugated process [9, 26]. Before turning to a derivation of CP violating asymmetries for the case of polarised final state leptons it is helpful to recall the unpolarised case.

3.1 Unpolarized decay spectrum

In the unpolarised case the CP -violating rate asymmetry can be defined by

$$A_{\text{CP}} = \frac{\Gamma_0 - \bar{\Gamma}_0}{\Gamma_0 + \bar{\Gamma}_0}, \quad (19)$$

where

$$\Gamma_0 \equiv \frac{d\Gamma}{d\hat{s}} \equiv \frac{d\Gamma(b \rightarrow dl^+l^-)}{d\hat{s}}, \quad \bar{\Gamma}_0 \equiv \frac{d\bar{\Gamma}}{d\hat{s}} \equiv \frac{d\Gamma(\bar{b} \rightarrow \bar{d}l^+l^-)}{d\hat{s}}. \quad (20)$$

The explicit expression for the unpolarized particle decay rate Γ_0 has been given in (11). Obviously, it can be written as a product of a real-valued function $r(\hat{s})$ times the function $\Delta(\hat{s})$, given in (12); $\Gamma_0(\hat{s}) = r(\hat{s}) \Delta(\hat{s})$. Taking the approach as in [9] we write the matrix elements for the decay and the anti-particle decay as

$$M = A + \lambda_u B, \quad \bar{M} = A + \lambda_u^* B, \quad (21)$$

where the CP-violating parameter λ_u , entering the Wilson coupling C_9^{eff} , has been defined in (5). Consequently, the rate for the anti-particle decay is then given by

$$\bar{\Gamma}_0 = \Gamma_0|_{\lambda_u \rightarrow \lambda_u^*} = r(\hat{s})\bar{\Delta}(\hat{s}) ; \quad \bar{\Delta} = \Delta|_{\lambda_u \rightarrow \lambda_u^*} . \quad (22)$$

Using (11) and (22), the CP violating asymmetry is evaluated to be [9]

$$A_{\text{CP}}(\hat{s}) = \frac{\Delta - \bar{\Delta}}{\Delta + \bar{\Delta}} = \frac{-2\text{Im}(\lambda_u)\Sigma}{\Delta + 2\text{Im}(\lambda_u)\Sigma} \simeq -2\text{Im}(\lambda_u)\frac{\Sigma(\hat{s})}{\Delta(\hat{s})} . \quad (23)$$

In (23),

$$\Sigma(\hat{s}) = \text{Im}(\xi_1^*\xi_2)[F_3(\hat{s}) + 6\hat{m}_l^2 F_1(\hat{s})] + 6\text{Im}(C_7^{\text{eff}}\xi_2)F_1(\hat{s})(1 + \frac{2\hat{m}_l^2}{\hat{s}}) . \quad (24)$$

In the presence of lepton l^- polarisation, the above CP asymmetry can get modified and receives a contribution from C_{10} through the interference piece with C_9^{eff} in $|M|^2$; see (16) and (18). In the following, we discuss this modification.

3.2 Polarized decay spectrum

In the polarised case, a CP violating asymmetry can be defined as follows

$$A_{\text{CP}}(\mathbf{n}) = \frac{\Gamma(\mathbf{n}) - \bar{\Gamma}(\bar{\mathbf{n}} = -\mathbf{n})}{\Gamma_0 + \bar{\Gamma}_0} , \quad (25)$$

where

$$\begin{aligned} \Gamma(\mathbf{n}) &\equiv \frac{d\Gamma(\hat{s}, \mathbf{n})}{d\hat{s}} \equiv \frac{d\Gamma(b \rightarrow dl^+l^-(\mathbf{n}))}{d\hat{s}} , \\ \bar{\Gamma}(\bar{\mathbf{n}}) &\equiv \frac{d\bar{\Gamma}(\hat{s}, \bar{\mathbf{n}})}{d\hat{s}} \equiv \frac{d\Gamma(\bar{b} \rightarrow d\bar{l}^+(\bar{\mathbf{n}})l^-)}{d\hat{s}} , \end{aligned} \quad (26)$$

and $\Gamma_0, \bar{\Gamma}_0$ have been defined in the previous section. Further, \mathbf{n} is the spin direction of the lepton l^- in the b -decay and $\bar{\mathbf{n}}$ is the spin direction of the l^+ in the \bar{b} -decay. For instance, assuming CP conservation, the rate for the decay of a B to a left handed electron should be the same as the rate for the decay of a \bar{B} to a right handed positron. More generally, in the CP conserving case, we would have

$$\Gamma(\mathbf{n}) \stackrel{CP \text{ cons.}}{=} \bar{\Gamma}(\bar{\mathbf{n}} = -\mathbf{n}) \Rightarrow A_{\text{CP}}(\mathbf{n}) = 0 . \quad (27)$$

The polarised decay spectrum for the b -decay has already been stated in (16). Using the above definitions the spectrum reads,

$$\Gamma(\mathbf{n}) = \frac{1}{2}\Gamma_0 (1 + P_i \mathbf{e}_i \cdot \mathbf{n}) , \quad (28)$$

where a sum over $i = L, T, N$ is implied. Analogously, for the corresponding CP conjugated process we have the decay spectrum

$$\bar{\Gamma}(\bar{\mathbf{n}}) = \frac{1}{2}\bar{\Gamma}_0 (1 + \bar{P}_i \bar{\mathbf{e}}_i \cdot \bar{\mathbf{n}}) . \quad (29)$$

Note that (28) and (29) *define* the polarisation asymmetries P_i and \bar{P}_i , respectively. With the choice $\bar{\mathbf{e}}_i = \mathbf{e}_i$, the \bar{P}_i are constructed from the decay spectrum in complete analogy to the P_i in (17). Moreover, from the condition $\Gamma(\mathbf{n}) = \bar{\Gamma}(\bar{\mathbf{n}} = -\mathbf{n})$, in the CP conserving case, it follows that $\bar{P}_i = -P_i$. In the general case we have

$$\bar{P}_i = -P_{i|\lambda_u \rightarrow \lambda_u^*} \quad (\text{for } \bar{\mathbf{e}}_i = \mathbf{e}_i) . \quad (30)$$

Now everything is at hand to calculate the CP violating asymmetries for a lepton l^- with polarisation $\mathbf{n} = \mathbf{e}_i$; inserting (28) and (29) into (25) one obtains the asymmetry,

$$\begin{aligned} A_{CP}(\mathbf{n} = \pm \mathbf{e}_i) &= \frac{1}{2} \left[\frac{\Gamma_0 - \bar{\Gamma}_0}{\Gamma_0 + \bar{\Gamma}_0} \pm \frac{\Gamma_0 P_i - (\Gamma_0 P_i)_{|\lambda_u \rightarrow \lambda_u^*}}{\Gamma_0 + \bar{\Gamma}_0} \right] \\ &= \frac{1}{2} \left[A_{CP}(\hat{s}) \pm \frac{\Delta P_i - (\Delta P_i)_{|\lambda_u \rightarrow \lambda_u^*}}{\Delta(\hat{s}) + \bar{\Delta}(\hat{s})} \right] \\ &\equiv \frac{1}{2} [A_{CP}(\hat{s}) \pm \delta A_{CP}^i(\hat{s})] , \quad i = L, T, N . \end{aligned} \quad (31)$$

On the r.h.s. of (31), $A_{CP}(\hat{s})$ is the unpolarized CP violating asymmetry given in (23). The polarised quantities $\delta A_{CP}^i(\hat{s})$ denote the modifications to the unpolarised spectra and will be stated explicitly below. It should be noted that for a given polarisation there are two independent observables, $A_{CP}(\mathbf{n} = \mathbf{e}_i)$ and $A_{CP}(\mathbf{n} = -\mathbf{e}_i)$ or, alternatively, $A_{CP}(\hat{s}) = A_{CP}(\mathbf{n} = \mathbf{e}_i) + A_{CP}(\mathbf{n} = -\mathbf{e}_i)$ (as it must be) and $\delta A_{CP}^i(\hat{s}) = A_{CP}(\mathbf{n} = \mathbf{e}_i) - A_{CP}(\mathbf{n} = -\mathbf{e}_i)$. The polarised CP violating asymmetries can be evaluated by inspecting the polarisation asymmetries in (18). After some algebra one finds the following final results:

$$\delta A_{CP}^i(\hat{s}) = \frac{-2\text{Im}(\lambda_u)\delta\Sigma^i(\hat{s})}{\Delta(\hat{s}) + 2\text{Im}(\lambda_u)\Sigma(\hat{s})} \simeq -2\text{Im}(\lambda_u)\frac{\delta\Sigma^i(\hat{s})}{\Delta(\hat{s})} , \quad (32)$$

with

$$\begin{aligned}
\delta\Sigma^L(\hat{s}) &= \text{Im}(C_{10}\xi_2) (1 + \hat{s} - 2\hat{s}^2) a , \\
\delta\Sigma^T(\hat{s}) &= \frac{3\pi\hat{m}_l}{2\sqrt{\hat{s}}}\lambda^{1/2}(1, \hat{s}, 0) \left[-2\text{Im}(C_7^{\text{eff}}\xi_2) + \frac{1}{2}\text{Im}(C_{10}\xi_2) - \hat{s}\text{Im}(\xi_1^*\xi_2) \right] , \\
\delta\Sigma^N(\hat{s}) &= \frac{3\pi\hat{m}_l}{2\sqrt{\hat{s}}}\lambda^{1/2}(1, \hat{s}, 0) \left[\frac{\hat{s}}{2}\text{Re}(C_{10}\xi_2) \right] a , \tag{33}
\end{aligned}$$

where a is the threshold factor defined in (11). It is interesting to note that the asymmetries, $\delta\Sigma^T(\hat{s})$ and $\delta\Sigma^N(\hat{s})$, have different combinations involving the imaginary and real parts of ξ_2 ; thereby, show dependence on the corrections to the four-quark operators, $O_1 - O_6$.

4 Numerical analysis and discussion

Having given the analytic framework for the various observables, we now turn to a discussion of our numerical results. We reiterate that these results are obtained following the discussions of section 2. In particular, we take in to account the $\rho - \omega$ resonance structure, which to our knowledge has so far been given little importance except in [9].

The basic and essential information is summarised in figures 1 to 4. In all our numerical estimates, we have used the parameters stated in the appendix. Furthermore, we have set $m_d = 0$ in our kinematic analysis as its dependence in $\Delta(\hat{s})$ (and similar kinematic factors) is negligible. On the other hand, the non-zero value for m_d given in the appendix has been used in evaluating the Wilson coupling C_9^{eff} . We have checked numerically that the use of small current masses $m_u = 2.3$ MeV and $m_d = 4.6$ MeV in the calculation of C_9^{eff} would result in appreciable changes of the asymmetries only in the region of the higher $c\bar{c}$ resonances ($\hat{s} > 0.5$) which is also affected by other theoretical uncertainties; see the discussion below. The theoretically clean region between the $\rho - \omega$ and the J/Ψ resonance remains almost unaffected.

The currently allowed range for the Wolfenstein parameters [27] is given in [28]; $0.190 < \rho < 0.268$, $0.284 < \eta < 0.366$. For our analysis we take $(\rho, \eta) = (0.25, 0.34)$. In terms of the Wolfenstein parameters, ρ and η , the

parameter λ_u is given by the relation,

$$\lambda_u = \frac{\rho(1-\rho) - \eta^2}{(1-\rho)^2 + \eta^2} - i \frac{\eta}{(1-\rho)^2 + \eta^2} + \dots \quad (34)$$

In Fig. 1, we display the branching ratios for the decay $b \rightarrow de^+e^-$ with unpolarized and longitudinally polarized electrons. The unpolarized branching ratio (solid line) has been obtained with help of (14). The corresponding results for polarised final state leptons have been calculated accordingly using (16). The dash-dotted and dotted lines corresponds to $\mathbf{n} = -\mathbf{e}_L$ and $\mathbf{n} = +\mathbf{e}_L$, respectively, where the unit vector \mathbf{e}_L has been defined in (15). As can be seen, in the SM, the decay is naturally left-handed and hence the polarised spectrum for $\mathbf{n} = -\mathbf{e}_L$ compares with the unpolarised spectrum. Whereas, the polarised $\mathbf{n} = \mathbf{e}_L$ spectrum is far below the unpolarised one; which according to our definition would correspond to a *wrong sign* decay. In the most relevant kinematical region, between the $\rho - \omega$ and $c\bar{c}$ resonances, the branching ratio is $\sim 3 \times 10^{-7}$. We would like to remind that this is theoretically the cleanest kinematic bin.

In Fig. 2, we present results for the polarised and unpolarised CP violating rate asymmetries calculated according to (31), (32), and (33) for the decay $b \rightarrow de^+e^-$. We find that the asymmetries for $b \rightarrow d\mu^+\mu^-$ are numerically similar to the results shown here, and hence are not presented. As mentioned earlier, only two of the shown four quantities are linearly independent. As can be observed, $A_{\text{CP}}(\mathbf{n} = -\mathbf{e}_L)$ is much larger than the asymmetry with opposite lepton polarization implying that $A_{\text{CP}}(\mathbf{n} = -\mathbf{e}_L)$ is quite similar to the unpolarized asymmetry A_{CP} ; the system is naturally polarized. This can be also seen by the lower half of Fig. 2 where the unpolarized A_{CP} and $(-1)\delta A_{\text{CP}}^L$ have been plotted. Here, $A_{\text{CP}}(\mathbf{n} = -\mathbf{e}_L)$ would be the average of the two curves (lying in the middle between them). Note that the polarised CP violating asymmetry δA_{CP}^L is comparable and in certain kinematic regions even larger than its unpolarized counterpart. Particularly, in the theoretically clean region, between the $\rho - \omega$ and the $c\bar{c}$ resonances, we find δA_{CP}^L is about 8% when compared to about 5% in the unpolarized case [9, 26]. However, in the resonance regions, the polarised asymmetry can reach values as large as up to 20% ($\rho - \omega$) and 11% ($c\bar{c}$), respectively.

A few other comments are in order. (i) In our analysis we have utilized the Wolfenstein parameters $(\rho, \eta) = (0.25, 0.34)$ which is in the experimentally

allowed range given above. However, the results for other values of these parameters can be easily obtained. Noticing that since $C_9^{\text{eff}}(\hat{s})$ only very weakly depends on ρ and η , almost the entire dependence is due the prefactors containing the CKM matrix elements; particularly, in the expressions for the branching ratio and the CP violating asymmetries. In the case of the branching ratio this is the term $|V_{tb}V_{td}^*/V_{cb}|^2 = \lambda^2[(1 - \rho)^2 + \eta^2]$; in the case of the CP violating asymmetries it is the factor $\text{Im}\lambda_u = -\eta/((1 - \rho)^2 + \eta^2)$. The results for other Wolfenstein parameters can therefore be obtained by simply rescaling the shown results. For instance varying (ρ, η) in the allowed range leads to a variation of $|\text{Im}\lambda_u|$ in the range $(0.54 \div 0.38)$. (For $(\rho, \eta) = (0.25, 0.34)$ we find $|\text{Im}\lambda_u| = 0.5$.) As can be seen the absolute value of the CP violating asymmetries increases with increasing ρ and η . On the other hand, the branching ratio mildly decreases with increasing ρ . (ii) Our results for A_{CP} in the region of the $\rho - \omega$ resonance are smaller than the values found in [9]. The discrepancy can most probably be traced back on the $\rho - \omega$ inelastic channel (see the function $G(s)$ in [29]) in which the absorptive part should be omitted below the inelastic threshold $\sqrt{s} < m_\pi + m_\rho$. On inclusion of the imaginary part also below this threshold, we find similarly large contributions at the $\rho - \omega$ resonances. (iii) In addition, the numerical results in the resonance region of the J/Ψ family are subject to theoretical uncertainties; usually denoted by a phenomenological factor κ_V which can vary between 2.35 to 1.00. For our numerical results we have set $\kappa_V = 1$. The variation of κ_V can affect the width and the CP asymmetry as has been discussed in [9].

The polarised asymmetries, $\delta A_{\text{CP}}^{\text{N}}$ and $\delta A_{\text{CP}}^{\text{T}}$, are proportional to the lepton mass and therefore only relevant in the case of final state tau leptons. In Fig. 3, branching ratios for the decay $b \rightarrow d\tau^+\tau^-$ are shown for unpolarized (solid line), longitudinally (dotted), normally (dashed), and transversely (dash-dotted) polarized taus. The corresponding branching ratio is $\sim \mathcal{O}(1 \times 10^{-8})$, requiring a larger luminosity. With tau leptons as final states, for $\mathbf{n} = \pm \mathbf{e}_{\text{N}}$; both rates are very similar, whereas, for $\mathbf{n} = \pm \mathbf{e}_{\text{T}}$, the $-\mathbf{e}_{\text{T}}$ state is strongly favored, as being closer to the unpolarised decay width. Therefore, we would classify the polarised $\mathbf{n} = \mathbf{e}_{\text{T}}$ spectra as a *wrong sign* decay.

In Fig. 4, we show both the polarised and unpolarised CP violating rate asymmetries calculated according to (31), (32), and (33) for the decay $b \rightarrow$

$d\tau^+\tau^-$. Since $\delta A_{\text{CP}}^{\text{L}}$ and $\delta A_{\text{CP}}^{\text{N}}$ are small we conclude that $A_{\text{CP}}(\mathbf{n} = +\mathbf{e}_{\text{L}}) \simeq A_{\text{CP}}(\mathbf{n} = -\mathbf{e}_{\text{L}})$ and $A_{\text{CP}}(\mathbf{n} = +\mathbf{e}_{\text{N}}) \simeq A_{\text{CP}}(\mathbf{n} = -\mathbf{e}_{\text{N}})$. On the other hand, $\delta A_{\text{CP}}^{\text{T}}$ is comparable to the unpolarised A_{CP} as is indicated by the dash-dotted line in the (2, 1)-panel. This in turn implies that $A_{\text{CP}}(\mathbf{n} = +\mathbf{e}_{\text{T}})$ is very small. As can be observed, all calculated asymmetries, reach at the maximum about 10%.

5 Summary

We have made a detailed study of the CP asymmetry for the process, $b \rightarrow dl^+l^-$, when one of the leptons is in a polarised state. Our results indicate that when a lepton is in a certain polarised state $(-\mathbf{e}_{\text{L}}, -\mathbf{e}_{\text{T}})$, the decay rates are comparable to the unpolarised spectrum. For the case of the normally polarised spectrum, both $\pm\mathbf{e}_{\text{N}}$ give similar widths but lower than in the case of $-\mathbf{e}_{\text{L}}$ and $-\mathbf{e}_{\text{T}}$. In the rest of the polarisation states, which we had defined to be the *wrong sign* states, the decay rates and the corresponding asymmetries are lower, in comparison to the unpolarised results. In the regions which are away from resonance, we find the polarised CP asymmetries are larger than the corresponding unpolarised asymmetry. As expected, the resonance regions show a large asymmetry and in all of our analysis, we have included the $\rho - \omega$ resonance states also. However, as discussed, the results at the resonance region suffer from theoretical uncertainties. Barring a small kinematic window, measuring A_{CP} requires d quark tagging (due to the dominant background $b \rightarrow sl^+l^-$) [9]; in addition, for the polarised asymmetries the polarization needs to be measured. However, within the SM given the left-handed nature of the interactions, for the case of the electron, it is dominantly in the $-\mathbf{e}_{\text{L}}$ state. We note that the results for the electron and muon in a given polarised state do not differ much and hence measuring a muon in a *wrong sign* polarised state $(+\mathbf{e}_{\text{L}})$ can be very sensitive to new physics. Essentially, we need to probe polarised $(+\mathbf{e}_{\text{L}})$ muons; which we expect to be possible by (i) angular distribution of the decay products and (ii) through the life time of the $+\mathbf{e}_{\text{L}}$ muons, which is enhanced as compared to the $-\mathbf{e}_{\text{L}}$ state due to the dynamics of the SM interaction (left-handed); this is also evident by their smaller decay width as observed in Fig. 1. The situation for the case of the tau leptons is different and we observe that the \mathbf{e}_{T} polarised state can be most sensitive to new physics (see Fig. 3). We note that the polarisation observables involve different quadratic combinations of the

Wilson couplings and hence make for additional consistency checks for the unpolarised SM decay spectra and also for a probe to new physics which can show in loop effects. In this respect, given a real valued C_{10} (for the SM), we note that the asymmetries, $\delta\Sigma^T$ and $\delta\Sigma^N$, can be of relevance through the contributions arising from the real and imaginary parts of the function ξ_2 to the operators, $O_1 - O_6$.

In order to observe a 3σ signal for $A_{CP}(\hat{s})$ about $\sim 10^{10}$ B mesons have been estimated to be required [9]. As already mentioned such a measurement requires a good d -quark tagging to distinguish it from the much more copious decay $b \rightarrow sl^+l^-$ and hence will be a challenging task at future hadronic colliders like LHCb, BTeV, ATLAS or CMS [30]. More dedicated experiments like Super-BABAR and Super-BELLE should be able to achieve this goal. BELLE and BABAR have already measured the rare decay $b \rightarrow sl^+l^-$ which could be measured with great accuracy at these high luminosity upgrades. Given enough statistics, and excellent kaon/pion identification, they may be able to measure $b \rightarrow dl^+l^-$ or the exclusive process $B \rightarrow \rho l^+l^-$.⁴ In contrast, for measuring $A_{CP}(\mathbf{n} = -\mathbf{e}_L)$ we need a similar number of produced B -mesons, provided an efficient polarisation measurement is possible, since the branching rates are very much alike as discussed previously. In this regard, given the almost massless nature of the electrons, the CP asymmetry for the decay $b \rightarrow de^+e^-$ would correspond to a polarised asymmetry as in (31). As a result, if our SM expectations for the asymmetry as calculated here (see Fig. 2) are not met with, we might have a reasonable chance to look for new physics in polarised decays. In this paper, we have classified all such polarised decays as *wrong sign* decays and these could be viable modes in search for new physics.

Acknowledgments

The work of Balaji has been supported by the Bundesministerium für Bildung, Wissenschaft, Forschung und Technologie, Bonn under contract no. 05HT1PEA9. Part of the work of I. S. has been done at the University of Dortmund supported by the 'Bundesministerium für Bildung und Forschung', Berlin/Bonn. We thank Frank Krüger and Lalit Sehgal for many useful discussions. I. S. thanks Matthias Steinhauser for helpful comments on the input parameters. We also thank E. Reya and A. Ali for comments and suggestions.

⁴We thank A. Ali for pointing this out to us.

A Input Parameters

$$\begin{aligned}m_b &= 4.8 \text{ GeV}, m_t = 165 \text{ GeV}, m_c = 1.3 \text{ GeV}, \\m_u &= m_d = m_\pi = 140 \text{ MeV}, \\m_e &= 0.511 \text{ MeV}, m_\mu = 0.106 \text{ GeV}, m_\tau = 1.777 \text{ GeV} \\ \mu &= m_b, B(B \rightarrow X_c e \bar{\nu}_e) = 10.4\% \\M_W &= 80.423 \text{ GeV}, M_Z = 91.1876 \text{ GeV}, \sin^2(\theta_W) = 0.23, \\ \alpha_{\text{em}} &= 1/129, \alpha_s(M_Z) = 0.1183, \Lambda_{\overline{\text{MS}}}^{(5)} = 230 \text{ MeV} \\ \lambda &= 0.2237, A = 0.8113, \rho = 0.25, \eta = 0.34\end{aligned}$$

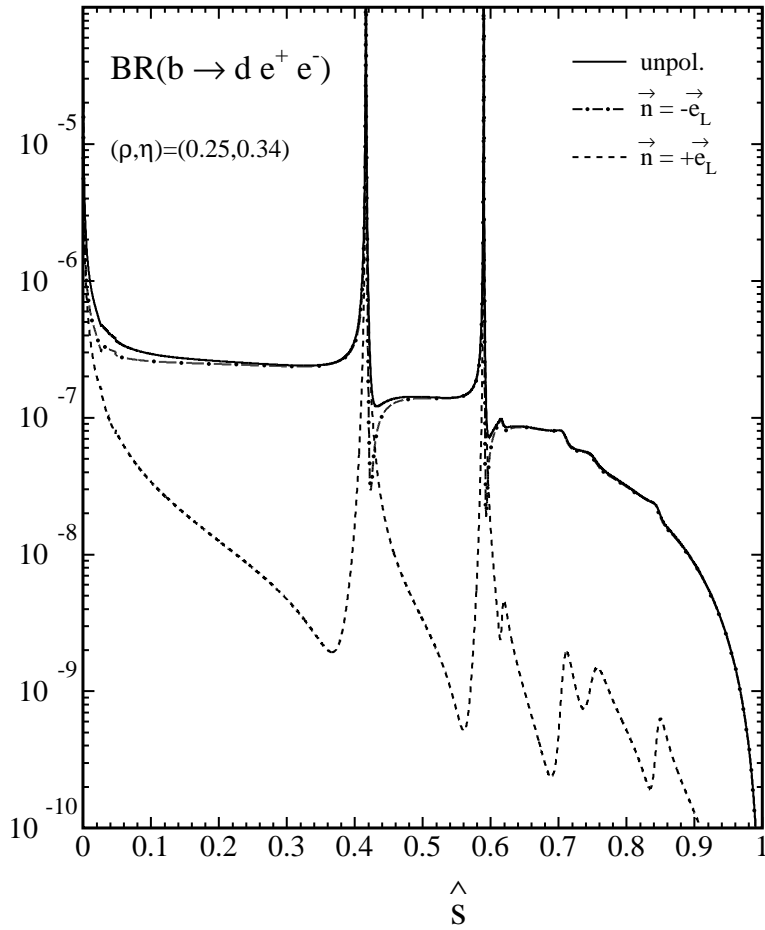


Figure 1: Polarised and unpolarised branching ratios for the decay $b \rightarrow d e^+ e^-$ according to (14) and (16). The unit vector \mathbf{e}_L has been defined in (15).

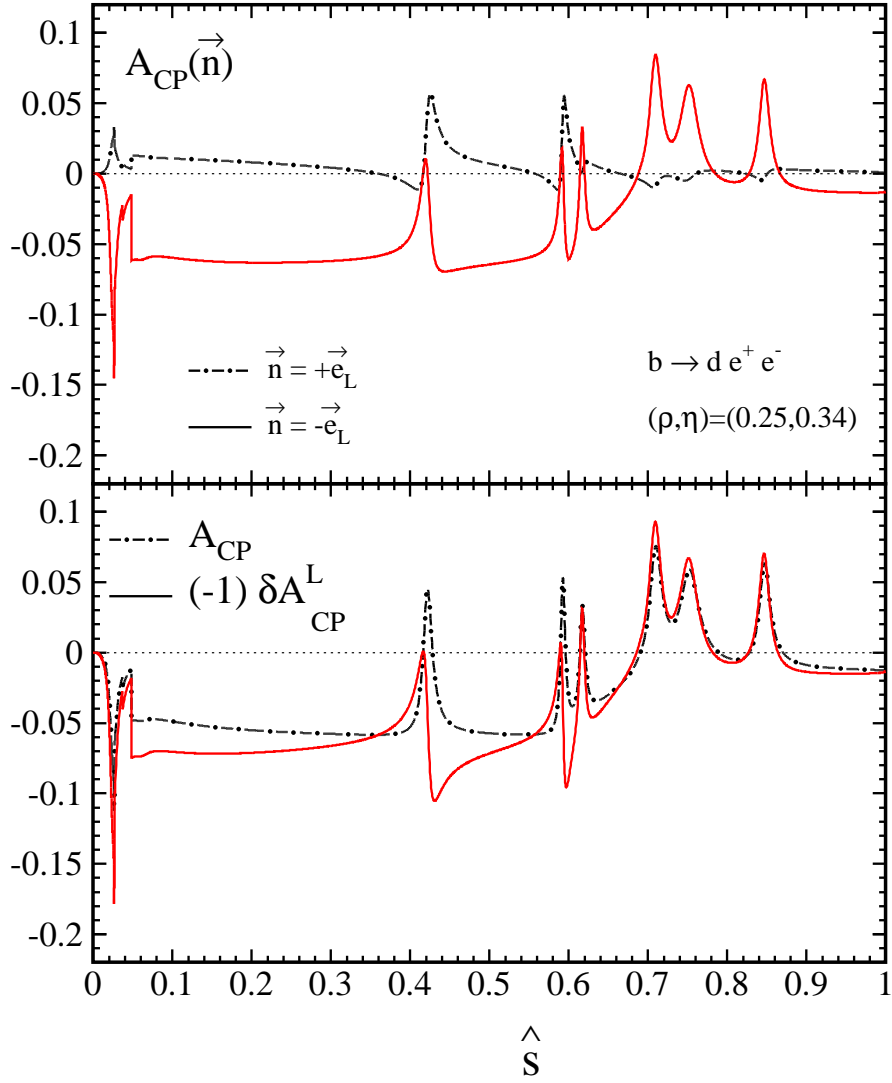


Figure 2: Polarised and unpolarised CP violating rate asymmetries for the decay $b \rightarrow d e^+ e^-$ as given in (31), (32) and (23), respectively.

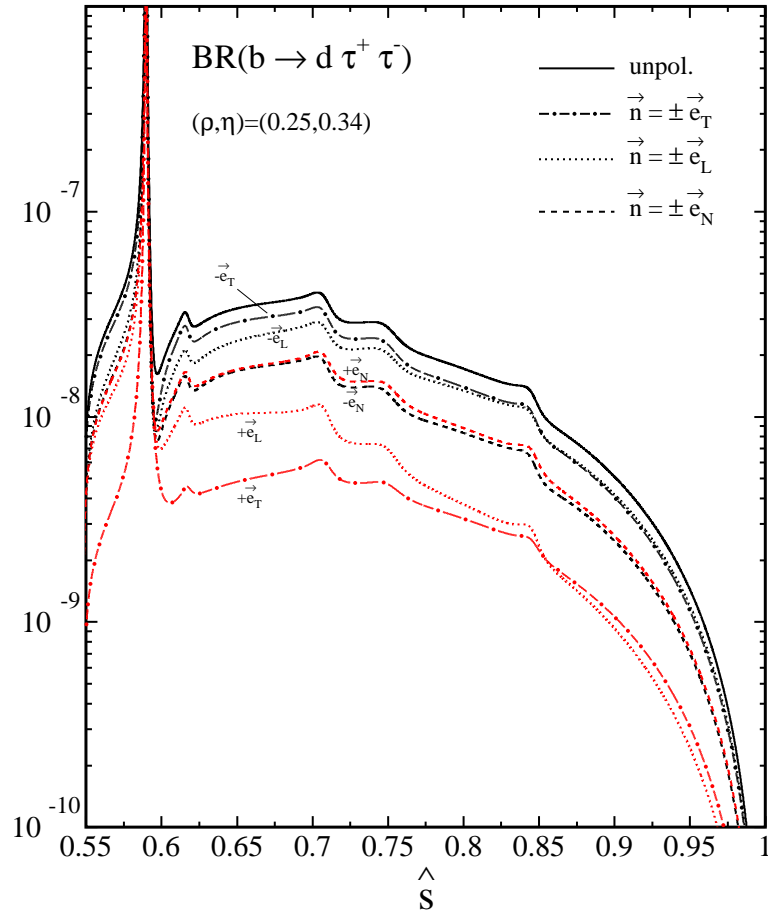


Figure 3: As in Fig. 1 for the decay $b \rightarrow d\tau^+\tau^-$.

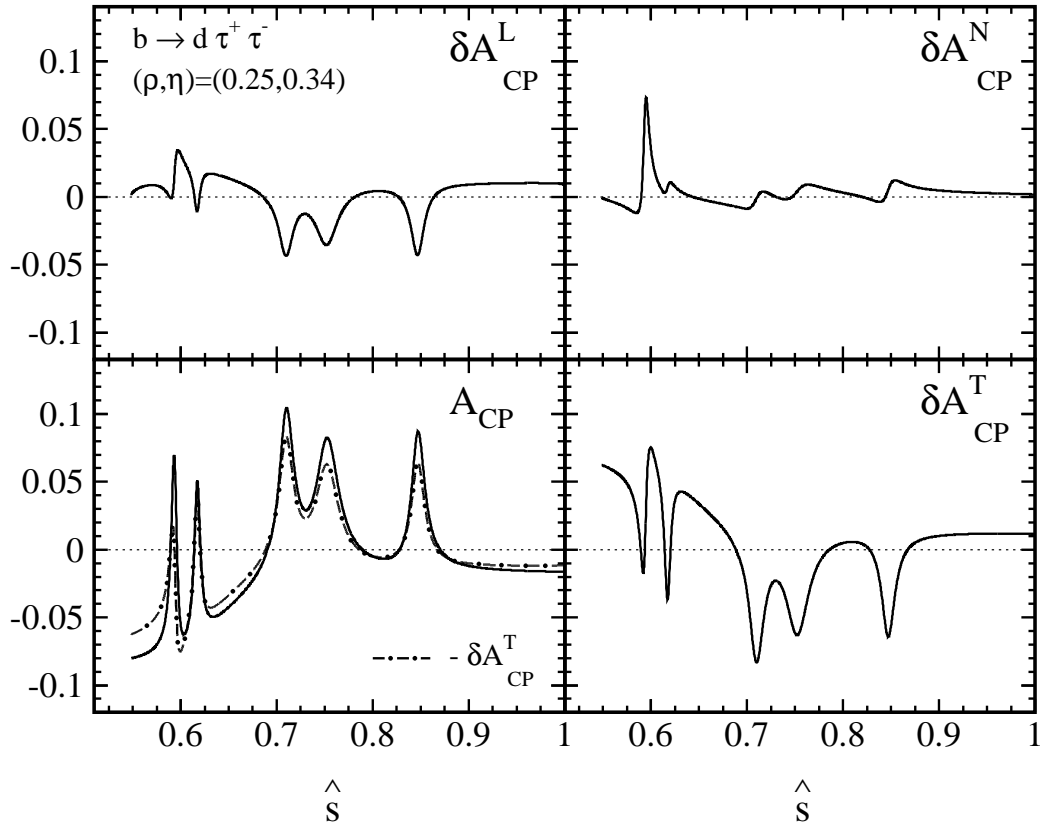


Figure 4: Polarised and unpolarised CP violating rate asymmetries for the decay $b \rightarrow d \tau^+ \tau^-$ as given in (32) and (23), respectively.

References

- [1] For a recent review, see A. J. Buras, hep-ph/0101336.
- [2] S. L. Glashow, J. Iliopoulos, and L. Maiani, Phys. Rev. **D2**, 1285 (1970).
- [3] M. S. Alam *et al.*, CLEO Collaboration, Phys. Rev. Lett. **74**, 2885 (1995).
- [4] R. Barate *et al.*, ALEPH Collaboration, Phys. Lett. **B429**, 169 (1998).
- [5] M. Neubert, Nucl. Phys. Proc. Suppl. **74**, 260 (1999).
- [6] N. G. Deshpande, J. Trampetic, and K. Panose, Phys. Rev. **D39**, 1461 (1989).
A. Ali and T. Mannel, Phys. Lett. **B264**, 447 (1991), (E) **B274**, 526 (1992).
C. Greub, A. Ioannisian, and D. Wyler, Phys. Lett. **B346**, 149 (1995).
D. Melikhov, N. Nikitin, and S. Simula, Phys. Lett. **B410**, 290 (1997).
W. Roberts, Phys. Rev. **D54**, 863 (1996).
C. Q. Geng and C. P. Kao, Phys. Rev. **D54**, 5636 (1996).
G. Burdman, Phys. Rev. **D57**, 4254 (1998).
- [7] E. Witten, Nucl. Phys. **B122**, 109 (1977).
- [8] B. Grinstein, M. J. Savage, and M. B. Wise, Nucl. Phys. **B319**, 271 (1989).
- [9] F. Krüger and L. M. Sehgal, Phys. Rev. **D55**, 2799 (1997).
- [10] See for example, D. Guetta and E. Nardi, Phys. Rev. **D58**, 012001 (1998).
- [11] S. Glenn *et al.*, CLEO Collaboration, Phys. Rev. Lett. **80**, 2289 (1998).
- [12] A. Ali, G. Hiller, L. T. Handoko, and T. Morozumi, Phys. Rev. **D55**, 4105 (1997).
- [13] J. Kaneko *et al.*, Belle Collaboration, hep-ex/0208029.

- [14] W. Bensalam, D. London, N. Sinha, and R. Sinha, Phys. Rev. **D67**, 034007 (2003).
- [15] A. J. Buras and M. Münz, Phys. Rev. **D52**, 186 (1995).
- [16] G. Buchalla, A. J. Buras, and M. E. Lautenbacher, Rev. Mod. Phys. **68**, 1125 (1996).
- [17] M. Misiak, Nucl. Phys. **B439**, 461(E) (1995).
- [18] J. Pumplin *et al.*, JHEP **07**, 012 (2002).
- [19] M. Jezabek and J. H. Kühn, Nucl. Phys. **B320**, 20 (1989).
- [20] C. S. Lim, T. Morozumi, and A. I. Sanda, Phys. Lett. **B218**, 343 (1989).
- [21] F. Krüger and L. M. Sehgal, Phys. Lett. **B380**, 199 (1996).
- [22] A. F. Falk, M. E. Luke, and M. J. Savage, Phys. Rev. **D49**, 3367 (1994).
- [23] A. Ali, T. Mannel, and T. Morozumi, Phys. Lett. **B273**, 505 (1991).
- [24] A. Ali, G. F. Giudice, and T. Mannel, Z. Phys. **C67**, 417 (1995).
- [25] J. L. Hewett, Phys. Rev. **D53**, 4964 (1996).
- [26] A. Ali and G. Hiller, Eur. Phys. J. **C8**, 619 (1999).
- [27] L. Wolfenstein, Phys. Rev. Lett. **51**, 1945 (1983).
L. Wolfenstein, Phys. Rev. Lett. **13**, 562 (1964).
- [28] D. Abbaneo *et al.*, *Combined results on b-hadron production rates and decay properties*, hep-ex/0112028.
- [29] T. Kinoshita, B. Nizic, and Y. Okamoto, Phys. Rev. **D31**, 2108 (1985).
- [30] N. Harnew, *The B physics potential of LHCb, BTeV, ATLAS and CMS*, Prepared for 8th International Symposium on Heavy Flavor Physics (Heavy Flavours 8), Southampton, England, 25-29 Jul 1999.